J|A|C|S ARTICLES

Published on Web 07/15/2009

CdSe Quantum Dot Sensitized Solar Cells. Shuttling Electrons Through Stacked Carbon Nanocups

Blake Farrow and Prashant V. Kamat*

Radiation Laboratory, Department of Chemistry and Biochemistry, University of Notre Dame, Notre Dame, Indiana 46556

Received April 26, 2009; E-mail: pkamat@nd.edu

Abstract: The charge separation between excited CdSe semiconductor quantum dots and stacked-cup carbon nanotubes (SCCNTs) has been successfully tapped to generate photocurrent in a quantum dot sensitized solar cell (QDSC). By employing an electrophoretic deposition technique we have cast SCCNT−CdSe composite films on optically transparent electrodes (OTEs). The quenching of CdSe emission, as well as transient absorption measurements, confirms ultrafast electron transfer to SCCNTs. The rate constant for electron transfer increases from 9.51×10^9 s^{-1} to 7.04×10^{10} s^{-1} as we decrease the size of CdSe nanoparticles from 4.5 to 3 nm. The ability of SCCNTs to collect and transport electrons from excited CdSe has been established from photocurrent measurements. The morphological and excited state properties of SCCNT−CdSe composites demonstrate their usefulness in energy conversion devices.

Introduction

The recent emergence of semiconductor quantum dots as light harvesters has stimulated a lot of interest in their use in next generation solar cell cells.[1] Due to the size quantization property one can readily tune the optical and electronic properties of the semiconductor materials and thus tune the response of quantum dot solar cells.[2−11] Creation of hot electrons and/or multiple exciton generation can further boost the performance of quantum dot based devices through high energy excitation.[12,13] Electron transfer between CdSe and other molecular systems has demonstrated the ability to shuttle electrons across the semiconductor interface.[14−18] Our recent work on quantum dot solar cells has demonstrated that CdSe quantum dots are able to sensitize TiO_2 particulate and tubular films by injecting electrons upon excitation with visible light.[2,11] Other strategies have also been considered in our laboratory to utilize II−VI semiconductor quantum dots in solar cells.[3,19,20]

To effectively gain energy from photogenerated excitons, the electron−hole pair must be quickly separated and the generated electron must have some means of transport to the electrode surface.[3,21] This is a major challenge impeding the development of next generation quantum dot based solar cells. Strategies to separate the charge carriers by means of another semiconductor,[2,4,5,7,17,22−31] metal nanoparticle,[9,32−34] or an electron acceptor shell[20] have been introduced to

(1) Kamat, P. V. *J. Phys. Chem. C* **2007**, *111*, 2834–2860.
(2) Kongkanand, A.; Tvrdy, K.; Takechi, K.; Kuno, M. K.; Kamat, P. V. *J. Am. Chem. Soc.* **2008**, *130*, 4007–4015.
(3) Kamat, P. V. *J. Phys. Chem. C* **2008**, *112*, 18737–18753.
(4) Leschkies, K. S.; Divakar, R.; Basu, J.; Enache-Pommer, E.; Boercker, J. E.; Carter, C. B.; Kortshagen, U. R.; Norris, D. J.; Aydil, E. S. *Nano Lett.* **2007**, *7*, 1793–1798.
(5) Mora-Sero, I.; Bisquert, J.; Dittrich, T.; Belaidi, A.; Susha, A. S.; Rogach, A. L. *J. Phys. Chem. C* **2007**, *111*, 14889–14892.
(6) Shen, Q.; Kobayashi, J.; Diguna. L. J.; Toyoda, T. *J. Appl. Phys.* **2008**, *103*, Art. No. 084304.
(7) Lee, H. J.; Yum, J.-H.; Leventis, H. C.; Zakeeruddin, S. M.; Haque, S. A.; Chen, P.; Seok, S. I.; Gratzel, M.; Nazeeruddin, M. K. *J. Phys. Chem. C* **2008**, *112*, 11600–11608.
(8) Weiss, E. A.; Porter, V. J.; Chiechi, R. C.; Geyer, S. M.; Bell, D. C.; Bawendi, M. G.; Whitesides, G. M. *J. Am. Chem. Soc.* **2008**, *130*, 83–92.
(9) Luther, J. M.; Law, M.; Beard, M. C.; Song, Q.; Reese, M. O.; Ellingson, R. J.; Nozik, A. J. *Nano Lett.* **2008**, *8*, 3488–3492.
(10) Jiang, X. M.; Schaller, R. D.; Lee, S. B.; Pietryga, J. M.; Klimov, V. I.; Zakhidov, A. A. *J. Mater. Res.* **2007**, *22*, 2204–2210.
(11) Bang, J. H.; Kamat, P. V. *ACS Nano* **2009**, doi: 10.1021/nn900324q.
(12) Schaller, R. D.; Agranovich, V. M.; Klimov, V. C. *Nat. Phys.* **2005**, *1*, 189–195.
(13) Ellingson, R. J.; Beard, M. C.; Johnson, J. C.; Yu, P.; Micic, O. I.; Nozik, A. J.; Shabaev, A.; Efros, A. L. *Nano Lett.* **2005**, *5*, 865–871.
(14) Sharma, S.; Pillai, Z. S.; Kamat, P. V. *J. Phys. Chem. B* **2003**, *107*, 10088–10093.
(15) Ginger, D. S.; Greenham, N. C. *Phys. Rev. B* **1999**, *59*, 10622–10629.
(16) Huang, J.; Stockwell, D.; Huang, Z. Q.; Mohler, D. L.; Lian, T. Q. *J. Am. Chem. Soc.* **2008**, *130*, 5632–5633.
(17) Harris, C. T.; Kamat, P. V. *ACS Nano* **2009**, *3*, 682–690.
(18) Vinayakan, R.; Shanmugapriya, T.; Nair, P. V.; Ramamurthy, P.; Thomas, K. G. *J. Phys. Chem. A* **2007**, *111*, 10146–10149.
(19) Baker, D. R.; Kamat, P. V. *Adv. Funct. Mater.* **2009**, *19*, 805–811.
(20) Brown, P.; Kamat, P. V. *J. Am. Chem. Soc.* **2008**, *130*, 8890–8891.
(21) Hodes, G. *J. Phys. Chem. C* **2008**, *112*, 17778–17787.
(22) Wijayantha, K. G. U.; Peter, L. M.; Otley, L. C. *Sol. Energy Mater. Solar Cells* **2004**, *83*, 363–369.
(23) Robel, I.; Subramanian, V.; Kuno, M.; Kamat, P. V. *J. Am. Chem. Soc.* **2006**, *128*, 2385–2393.
(24) Gur, I.; Fromer, N. A.; Geier, M. L.; Alivisatos, A. P. *Science* **2005**, *310*, 462–464.
(25) Yu, P.; Zhu, K.; Norman, A. G.; Ferrere, S.; Frank, A. J.; Nozik, A. J. *J. Phys. Chem. B* **2006**, *110*, 25451–25454.
(26) Niitsoo, O.; Sarkar, S. K.; Pejoux, C.; Ruhle, S.; Cahen, D.; Hodes, G. *J. Photochem. Photobiol. A* **2006**, *181*, 306–313.
(27) Tachibana, Y.; Akiyama, H. Y.; Ohtsuka, Y.; Torimoto, T.; Kuwabata, S. *Chem. Lett.* **2007**, *36*, 88–89.
(28) Diguna, L. J.; Shen, Q.; Kobayashi, J.; Toyoda, T. *Appl. Phys. Lett.* **2007**, *91*, Art. No. 023116.
(29) Lee, W.; Lee, J.; Lee, S.; Yi, W.; Han, S. H.; Cho, B. W. *Appl. Phys. Lett.* **2008**, *92*, Art. No. 153510.
(30) Mora-Seró, I.; Giménez, S.; Moehl, T.; Fabregat-Santiago, F.; Lana-Villareal, T.; Gómez, R.; Bisquert, J. *Nanotechnology in Mesostructured Materials* **2008**, *19*, 424007.
(31) Guijarro, N.; Lana-Villarreal, T.; Mora-Seró, I.; Bisquert, J.; Gómez, R. *J. Phys. Chem. C* **2009**, *113*, 4208–4214.

10.1021/ja903337c CCC: $40.75

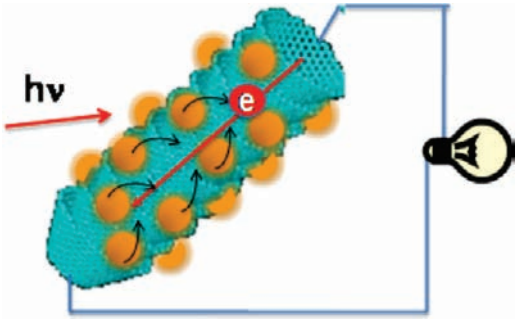

Figure 1. Illustration of stacked-cup carbon nanotube (SCCNT) based solar cell. The "open-cup" structure provides a tubular carbon structure with many open functionalization sites.

enhance the operation of quantum dot solar cells. Photoinduced charge transfer dynamics in type-II CdSe/CdTe donor−acceptor nanorods has been shown to occur on a 500 fs time scale.[35] The charge transport within the nanostructure film also plays an important role in dictating overall photoconversion efficiency. Nanotubes and other 1-D architectures have been found to be effective in improving the charge transport within the several micrometer thick photoactive film.[2,4,19,36−38]

Carbon nanostructures can serve as building blocks in light harvesting architectures[1,39−41] because of their unique electronic and optical properties. For example, semiconducting single-walled carbon nanotubes (SWCNTs) and stacked-cup carbon nanotubes (SCCNTs) have been shown to exhibit photovoltaic properties.[42,43] SCCNTs have been successfully utilized to capture and transport electrons from donor species such as porphyrin.[40] Electrons injected into SWCNT networks have been shown to survive over a very long time scale (minutes−hours).[44,45] This property has been exploited to capture photogenerated electrons and transport them to the electrode surface in CdS−SWCNT and TiO_2−SWCNT based solar cells.[46]

SCCNTs, as depicted in Figure 1, are nanofibers with a stacking morphology of truncated conical graphene layers (cups). They exhibit a large portion of open edges on the rim of each cup, thus making a large area available for chemical functionalization. We have now employed an SCCNT network as conducting scaffolds to anchor CdSe quantum dots for light harvesting in a photoelectrochemical solar cell. By combining the properties of exciton generation in CdSe quantum dots[47] and the electron capture and transport characteristics of SCCNTs, we have succeeded in developing an effective strategy for harvesting light energy through SCCNT−CdSe composites. The excited state interactions between SCCNT and CdSe and the charge transfer processes leading to the generation of photocurrent are also described herein.

Experimental Section

CdSe quantum dots were synthesized using the procedure described in literature.[48] This preparation resulted in monodisperse CdSe quantum dots with diameters ranging from 3 to 4.5 nm with a capping of trioctylphosphine oxide (TOPO) that are easily suspendable in toluene or other nonpolar solvents. The stacked-cup carbon nanotubes (SCCNTs) were obtained as gift samples from CGI Creos Corporation of Japan and were readily suspendable in THF and other polar solvents within 30−60 min of sonication.

The SCCNT−CdSe composites were prepared by simultaneous injection of the two suspensions (viz. SCCNT and CdSe) into a pool of acetonitrile. Addition of one part SCCNT in THF (0.2 mg/mL) and one part 5 μM CdSe quantum dot solution in toluene to four parts acetonitrile quickly changes the bright orange color of the quantum dot solution to a grayish brown suspension. To ensure even distribution of the particles and to reduce flocculation of the SCCNTs, the resulting solution was sonicated for 10−20 min. Under black light (UV) illumination the unmixed CdSe solution emits brightly, but after mixing with SCCNT solution the emission is quenched. It is expected that the TOPO capping on the CdSe quantum dots facilitates binding of CdSe to the SCCNT in solution in two different ways. First, the SCCNT structure has many openings in the sp^2 carbon lattice where the open-cup structures terminate, creating a ring of functional groups, including carboxylic acids. Efforts have been made to use such functionalization to graft the carbon surfaces or to attach Pt nanoparticles.[49−52] Such functional groups are likely to assist binding of CdSe nanocrystals. Second, the long hydrophobic tails on the TOPO capping of the CdSe dot will experience an attraction to the large hydrophobic area of the graphitic sheets on the SCCNTs.

Electrophoretic Deposition. We utilized an electrophoretic deposition method to cast films of the composites onto optically transparent electrodes. The optically transparent electrodes (OTEs) used were indium-doped tin oxide (ITO) coated glass with a spin-coated nanostructured SnO_2 film cast and annealed on the surface. The electrophoretic deposition method has been utilized before to cast robust thin films of semiconducting quantum dots,[20] SWCNTs,[36] and SCCNTs.[43] Approximately 2 mL of SCCNT−CdSe composite suspension (prepared using the methodology in the previous section) were placed in a 1 cm cuvette. Two SnO_2/OTE electrodes were inserted 5 mm apart, and a 300 V/cm DC field was applied. Within a minute the solution between the electrodes became colorless, as a robust thin film composed of SCCNT−CdSe

(32) Pons, T.; Medintz, I. L.; Sapsford, K. E.; Higashiya, S.; Grimes, A. F.; English, D. S.; Mattoussi, H. *Nano Lett.* **2007**, *7*, 3157–3164.
(33) Koleilat, G. I.; Levina, L.; Shukla, H.; Myrskog, S. H.; Hinds, S.; Pattantyus-Abraham, A. G.; Sargent, E. H. *ACS Nano* **2008**, *2*, 833–840.
(34) Gross, D.; Susha, A. S.; Klar, T. A.; Da Como, E.; Rogach, A. L.; Feldmann, J. *Nano Lett.* **2008**, *8*, 1482–1485.
(35) Dooley, C. J.; Dimitrov, S. D.; Fiebig, T. *J. Phys. Chem. A* **2008**, *112*, 12074–12076.
(36) Robel, I.; Bunker, B.; Kamat, P. V. *Adv. Mater.* **2005**, *17*, 2458–2463.
(37) Chen, S. G.; Paulose, M.; Ruan, C.; Mor, G. K.; Varghese, O. K.; Kouzoudis, D.; Grimes, C. A. *J. Photochem. Photobiol. A* **2006**, *177*, 177–184.
(38) Shankar, K.; Basham, J. I.; Allam, N. K.; Varghese, O. K.; Mor, G. K.; Feng, X.; Paulose, M.; Seabold, J. A.; Choi, K.-S.; Grimes, C. A. *J. Phys. Chem. A* **2009**, *113*, 6327–6359.
(39) Kamat, P. V. *Nanotoday* **2006**, *1*, 20–27.
(40) Hasobe, T.; Kamat, P. V. *J. Phys. Chem. C* **2007**, *111*, 16626–16634.
(41) Avouris, P. *Acc. Chem. Res.* **2002**, *35*, 1026–1034.
(42) Barazzouk, S.; Hotchandani, S.; Vinodgopal, K.; Kamat, P. V. *J. Phys. Chem. B* **2004**, *108*, 17015–17018.
(43) Hasobe, T.; Fukuzumi, S.; Kamat, P. V. *Angew. Chem., Int. Ed.* **2006**, *45*, 755–759.
(44) Kongkanand, A.; Kamat, P. V. *J. Phys. Chem. C* **2007**, *111*, 9012–9015.
(45) Khairoutdinov, R. F.; Doubova, L. V.; Haddon, R. C.; Saraf, L. *J. Phys. Chem. B* **2004**, *108*, 19976–19981.
(46) Kongkanand, A.; Domínguez, R. M.; Kamat, P. V. *Nano Lett.* **2007**, *7*, 676–680.
(47) Robel, I.; Kuno, M.; Kamat, P. V. *J. Am. Chem. Soc.* **2007**, *129*, 4136–4137.
(48) Peng, Z. A.; Peng, X. *J. Am. Chem. Soc.* **2001**, *123*, 183–184.
(49) Colavita, P. E.; Streifer, J. A.; Sun, B.; Wang, X. Y.; Warf, P.; Hamers, R. J. *J. Phys. Chem. C* **2008**, *112*, 5102–5112.
(50) Colavita, P. E.; Sun, B.; Tse, K. Y.; Hamers, R. J. *J. Am. Chem. Soc.* **2007**, *129*, 13554–13565.
(51) Marcus, M. S.; Shang, L.; Li, B.; Streifer, J. A.; Beck, J. D.; Perkins, E.; Eriksson, M. A.; Hamers, R. J. *Small* **2007**, *3*, 1610–1617.
(52) Metz, K. M.; Goel, D.; Hamers, R. J. *J. Phys. Chem. C* **2007**, *111*, 7260–7265.

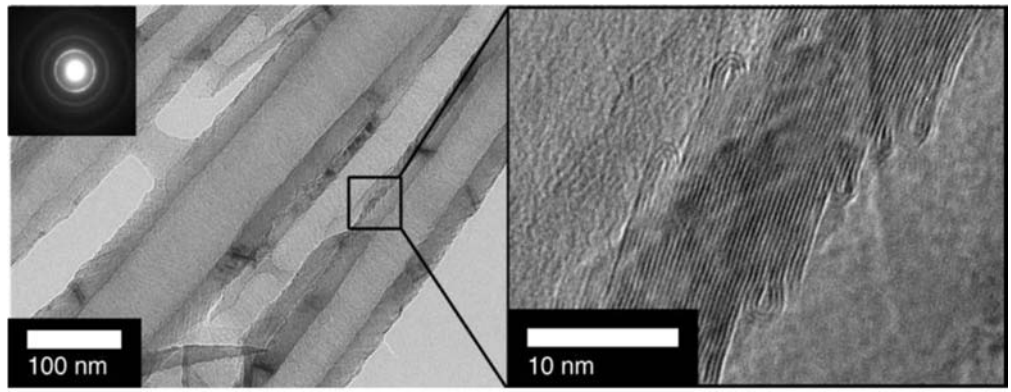

Figure 2. HRTEM image of a group of three stacked-cup carbon nanotubes (Left). The enlarged area (right) shows a cross section of one side of the open-cup shell composed of stacked graphitic sheets. Inset shows selected area electron diffraction (SAED) of a single SCCNT.

was deposited on the positively charged electrode. Earlier methods employed different dc fields to cast CdSe quantum dot films (~80 V/cm) as well as SCCNT films (~200 V/cm) as described in literature.[20,43] The differences in the strength of the DC field required can be attributed to the dielectric media and surface charging on the electrodes.

Experimental Setup. UV−visible absorption spectra were recorded using a Cary 50 Bio UV−visible spectrophotometer. Emission spectra were recorded using an SLM-S 8000 spectrofluorometer. Emission lifetimes of films and solutions were measured using a Horiba Jobin Yvon single photon counting system with a 373 nm, 1 MHz repetition rate, 1.1 ns pulse width diode source. Photoelectrochemical measurements were made using a Keithley 2601 programmable electrometer and a two electrode cell using platinum gauze as the counter electrode and a 0.1 M Na_2S redox couple. The experiments were conducted using a 150 W xenon lamp with a >300 nm $CuSO_4$ filter as the light source. A Bausch and Lomb high intensity monochromator (fwhm ~15 nm) and a Keithley 617 programmable electrometer were utilized for IPCE (Incident photon conversion efficiency) measurements. Scanning Electron Microscope (SEM) images were obtained using a Hitachi S-4500 FESEM. Transmission Electron Microscope (TEM) images were obtained using a JEOL 2010 TEM. Time resolved transient absorption spectra were recorded using a TA spectrometer with femtosecond resolution. The laser used for excitation was a Clark MXR-2010 Ti:Sapphire laser system capable of 775 nm laser pulses of 1 mJ/pulse (width of 150 fs) at a rate of 1 kHz. A fraction (5%) of the beam was used to generate a probe pulse. The second harmonic (387 nm) was used for excitation of the sample.

Results and Discussion

Characterization of SCCNTs. Stacked-cup carbon nanotubes (SCCNTs) are a class of carbon nanostructures with a tubular morphology but differ significantly from SWCNT structures. While SWCNTs are composed of a seamless sp^2 carbon nanotube, SCCNTs are composed of a series of curled graphene-like sheets that form an "open-cup" shape and stack successively in a close-packed tubular morphology.[43,53−56] SWCNTs are often difficult to functionalize without degradation of electronic characteristics because the addition of functional groups along their length breaks the seamless carbon lattice. The "open-cup" structure of SCCNTs creates inner and outer reactive edges along the length of the tube both inside and out, allowing ease of functionalization while preserving the conductive graphitic stacking within the tube.

Figure 2 shows high resolution TEM images of SCCNTs at two different magnifications. These fibers consist of stacked cups with open rings, as seen in the HRTEM image. It is evident from these images that the tubes are constructed out of successively stacked graphitic sheets with a sheet spacing of approximately 3.4 Å. This spacing is similar to that of graphene spacing in graphite, and it agrees well with the estimated values for stacked-carbon nanocones.[57]

Electrophoretic Deposition of SCCNT and SCCNT−CdSe Films. As shown earlier, SCCNT and CdSe films can be deposited on conducting electrode surfaces using an electrophoretic deposition technique.[20,43] Both CdSe and SCCNT and their composite carry a net charge when suspended in a solvent mixture that contains a small amount of polar solvent such as acetonitrile. When subjected to a dc electric field, they quickly migrate to the electrode and get deposited as a uniform film. The films obtained by the electrophoretic deposition method are quite robust and are suitable for spectroscopic and photoelectrochemical measurements.

The SCCNT−CdSe composite films were prepared by mixing the suspensions of SCCNT and CdSe nanocrystals in a known proportion of THF/toluene/acetonitrile (1:1:4 v/v/v) mixed solvent and carrying out electrophoretic deposition, as described in the experimental section. The films obtained by this method showed uniform coverage on OTEs and were robust for microscopy and photoelectrochemical measurements. Figure 3 shows SEM images of SCCNT films cast on OTEs in the absence and presence of CdSe quantum dots. SEM images of the electrophoretically cast films show a network of several micrometer long SCCNTs over the electrode surface. This network of SCCNTs is expected to serve as a conducting scaffold to capture and transport photogenerated charge carriers.

The SCCNTs in the composite films (Figure 3) show a dense coverage of CdSe nanocrystals. The excess CdSe nanocrystals appear to fill in the void spaces of the SCCNT network. As can be seen in the HRTEM image in Figure 4, the CdSe quantum dots exist both on the surface of the stacked-cup tubes and away from the surface. The close packing of the CdSe nanocrystals at the SCCNT surface is of interest due to their excited state interactions. The CdSe nanocrystals away from SCCNT surface

(53) Endo, M.; Kim, Y. A.; Ezaka, M.; Osada, K.; Yanagisawa, T.; Hayashi, T.; Terrones, M.; Dresselhaus, M. S. *Nano Lett.* **2003**, *3*, 723–726.
(54) Endo, M.; Kim, Y. A.; Hayashi, T.; Fukai, Y.; Oshida, K.; Terrones, M.; Yanagisawa, T.; Higaki, S.; Dresselhaus, M. S. *Appl. Phys. Lett.* **2002**, *80*, 1267–1269.
(55) Kim, C.; Kim, Y. J.; Kim, Y. A.; Yanagisawa, T.; Park, K. C.; Endo, M.; Dresselhaus, M. S. *J. Appl. Phys.* **2004**, *96*, 5903–5905.
(56) Kim, Y. A.; Hayashi, T.; Fukai, Y.; Endo, M.; Yanagisawa, T.; Dresselhaus, M. S. *Chem. Phys. Lett.* **2002**, *355*, 279–284.
(57) Gogotsi, Y.; Dimovski, S.; Libera, J. A. *Carbon* **2002**, *40*, 2263–2267.

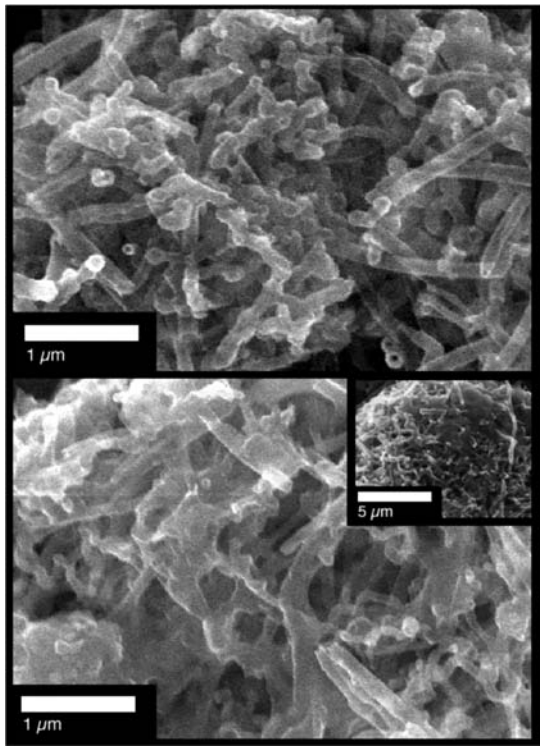

Figure 3. SEM images of a SCCNT cluster without (top) and with (bottom and inset) CdSe quantum dots. Bottom image shows the coating of the CdSe on the tube surface while the inset image is zoomed out for clarity and context.

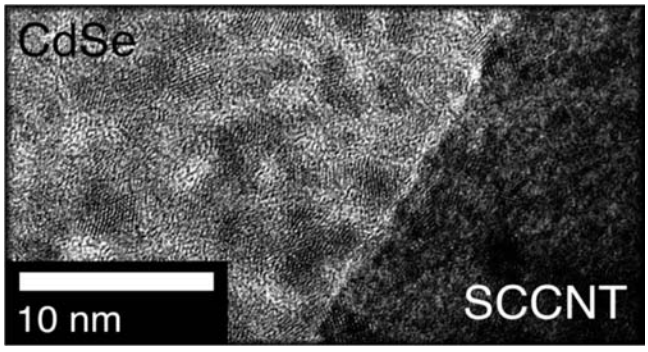

Figure 4. HRTEM image of the CdSe quantum dot−SCCNT interface. CdSe quantum dots with ~3 nm diameter cluster around the surface of a stacked-cup carbon nanotube.

exhibit diffraction patterns that are characteristic of 3 nm diameter CdSe quantum dots. It is this proximity as well as the low Fermi level of the stacked cups that allows for easy electron transfer between the excited quantum dot and the SCCNT surface.

Absorption Characteristics. The absorption spectra of pristine CdSe quantum dots in toluene solution are shown in Figure 5B. The three different size particles of approximate diameter 3, 4, and 4.5 nm used in the present investigation show the size quantization effects with characteristic exciton bands at 498, 547, and 570 nm, respectively. The absorption spectra of SCCNT−CdSe shown in Figure 5A confirm that the original absorption properties of the CdSe quantum dots are retained. The absorption spectra shown in the inset of Figure 5A represent absorbance corresponding to both SCCNT and CdSe nanocrystals. The unadjusted absorbance spectra of the composite films (shown in Figure 5A, inset) include a contribution from SCCNT absorbance. The SCCNTs absorb fairly uniformly throughout the visible spectrum, with absorbance ranging from 0.6 to 0.5 optical density in the range 500−600 nm. To exclude the absorption of SCCNTs, we separately recorded SCCNT films without CdSe incorporation. The spectra recorded after SCCNT background subtraction show the excitonic features of corresponding CdSe nanocrystals in the SCCNT−CdSe films. These absorption features confirm that the native properties of CdSe nanocrystals are retained in the composite films.

Probing Excited State Interactions. CdSe quantum dots are highly emissive as the photogenerated charge carriers undergo radiative recombination. Emission quantum yields as high as 80% have been achieved for quantized CdSe nanocrystals.[3] The emission spectrum of 4.5 nm diameter CdSe quantum dots (Figure 6A) shows an emission peak around 590 nm. Upon addition of SCCNTs we observe a dramatic quenching of the emission. Nearly 95% quenching of CdSe emission by SCCNTs observed in the composite film is indicative of the fact that radiative decay becomes a minor pathway. Because of the interference from the absorption of SCCNTs at the excitation wavelength, it is rather difficult to obtain a quantitative estimate of quenching of CdSe emission. To further establish the quenching process we monitored the emission decay of CdSe and SCCNT−CdSe in solution. (Figure 6B)

We probed the excited state interactions in the films by recording the emission decay of CdSe and SCCNT−CdSe films that were cast on OTEs by electrophoretic deposition. The emission decay traces in Figure 7 confirm the quenching of CdSe emission by SCCNTs. Based on the results presented in Figures 6 and 7 we can conclude that an additional nonradiative pathway competes with the fluorescence of excited CdSe dots. As demonstrated in previous studies, such emission quenching represents electron transfer at the semiconductor surface.[58] In the present experiments we expect SCCNTs to serve as an electron acceptor and thus compete with the radiative recombination (eqs 1 and 2).

$$\mathrm{CdSe} + h\nu \rightarrow \mathrm{CdSe}(e^- + h^+) \rightarrow \mathrm{CdSe} + h\nu' \quad (1)$$

$$\mathrm{CdSe}(e^- + h^+) + \mathrm{SCCNT} \rightarrow \mathrm{CdSe}(h^+) + \mathrm{SCCNT}(e^-) \quad (2)$$

The hole remaining in CdSe can recombine with the SCCNT (e^-) or induce anodic corrosion.[58] The emission decay was analyzed using biexponential decay kinetics, and the results are summarized in the Supporting Information. The average lifetime of 4.5 nm CdSe quantum dots was 8.11 ns; however, in the SCCNT−CdSe composite film the lifetime decreased to 0.93 ns. A similar decrease in lifetime was also observed for 3 and 4 nm CdSe nanocrystals. It should be noted that the charge transfer events occur over a wide range of time scales, and emission lifetime analysis captures events that occur in the slow (nanosecond) time scale. From Figure 7 it is also evident that most of the quenching occurs on a fast time scale and, because of the laser pulse width limitation, we could not resolve this component from the emission decay.

To probe the ultrafast electron transfer between the excited quantum dot and SCCNT in the subnanosecond time scale, we employed femtosecond transient absorption spectroscopy by suspending CdSe and SCCNT−CdSe composites in a THF/toluene/acetonitrile mixture. The transient absorption spectra recorded at different times following the 387 nm laser pulse

(58) Tvrdy, K.; Kamat, P. V. *J. Phys. Chem. A* **2009**, *113*, 3765–3772.

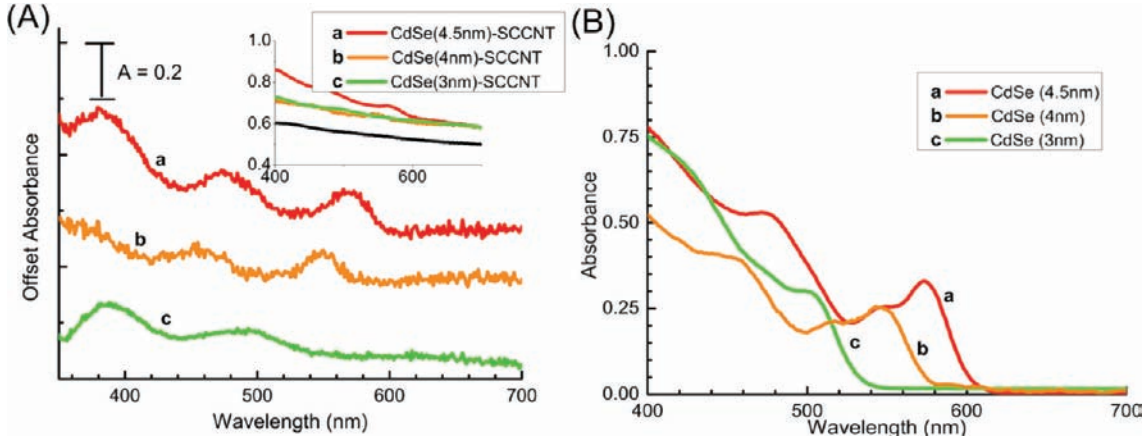

Figure 5. (A) UV−visible absorption spectra of three different sized CdSe quantum dot−SCCNT hybrid structure films. Main plot: SCCNT film used as baseline and spectra offset for clarity. Inset: Absorbance spectra of uncorrected SCCNT−CdSe (a−c) and SCCNT (black line) films. (B) UV−visible absorption spectra of three different sized quantum dots in toluene used in present experiments.

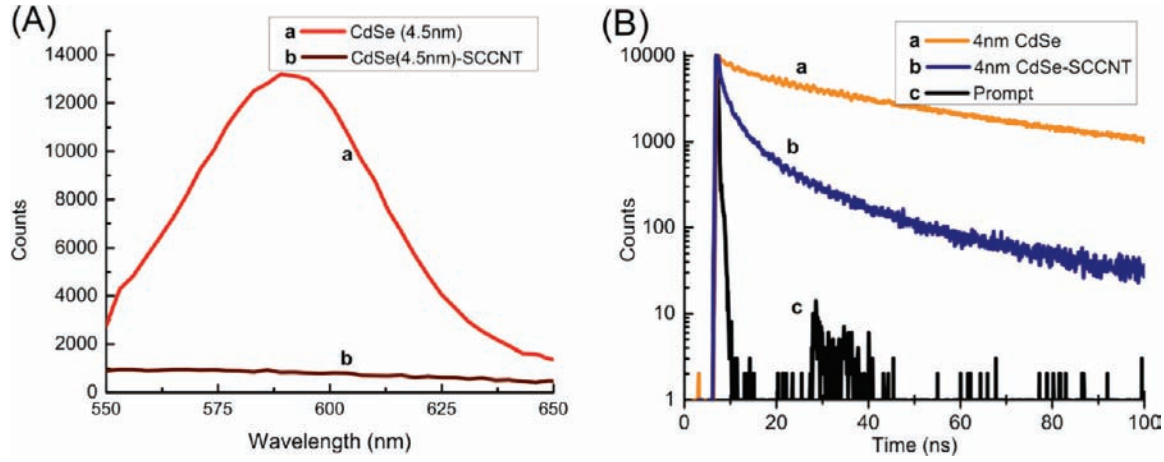

Figure 6. (A) Fluorescence emission spectra of CdSe and SCCNT−CdSe in toluene−acetonitrile. Excitation was set to 373 nm. (B) Emission decay at 547 nm recorded using excitation at 373 nm diode laser: (a) CdSe quantum dots as prepared in toluene; (b) CdSe-SCCNT suspension in THF/toluene/acetonitrile (1:1:4 v/v/v).

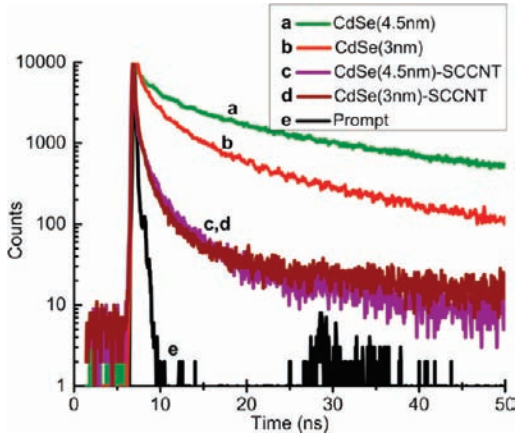

Figure 7. Emission decay of CdSe thin films cast on (a, b) OTEs and (c, d) SCCNT−CdSe films cast on OTE/SnO_2. The emission was monitored at (a, c) 590 nm and (b, d) 515 nm using 373 nm excitation. Trace e represents scatter of laser pulse.

excitation of CdSe and SCCNT−CdSe are shown in Figure 8. As discussed earlier,[58] the transient bleaching, which represents charge separation within the CdSe nanocrystals, recovers over a period of several nanoseconds to occur at a faster rate. Quick removal of one of the charge carriers by an acceptor species causes the bleaching recovery.

In the present experiments we recorded the bleaching recovery for 3, 4, and 4.5 nm CdSe nanocrystals at the corresponding bleaching maximum. Representative recovery traces for the three diameters of CdSe quantum dots recorded at 498, 547, and 570 nm are shown in Figure 9. In the absence of SCCNTs, the bleaching recovery of different diameter CdSe quantum dots exhibits size dependency. Smaller size CdSe quantum dots show a faster bleaching during the first few picoseconds following laser pulse excitation. The higher surface-to-volume ratio for smaller sized quantum dots is expected to influence the intrinsic decay kinetics.

In the presence of SCCNTs the recovery becomes faster as the electrons are transferred across the interface (the reaction shown in eq 2). These recovery traces exhibit multiexponential behavior and can be fitted to biexponential kinetics using eq 3.

$$F(t) = a_1 e^{-t/\tau_1} + a_2 e^{-t/\tau_2} \quad (3)$$

For comparison purposes, we have determined the average lifetimes using eq 4.[59]

(59) James, D. R.; Liu, Y.-S.; de Mayo, P.; Ware, W. R. *Chem. Phys. Lett.* **1985**, *120*, 460.

$$\langle\tau\rangle = \frac{\sum(a_i\tau_i^2)}{\sum(a_i\tau_i)} \quad (4)$$

The results of the kinetic analysis are summarized in Table 1.

For CdSe alone we observed relatively long-lived bleaching recovery with average lifetimes of 62, 59, and 39 ps for 4.5, 4, and 3 nm diameter particles, respectively. A decrease in the average CdSe bleaching recovery lifetime was evident when bound to the SCCNT surface with corresponding average lifetimes of 39, 34, and 10 ps for 4.5, 4, and 3 nm diameter CdSe nanocrystals, respectively. If we consider the decrease in lifetime as being due to the electron transfer to SCCNTs, we can obtain the electron transfer rate constant from eq 5.

$$k_{et} = (1/\tau' - 1/\tau_0) \quad (5)$$

where τ' and τ_0 correspond to the average lifetime of bleaching recovery in the presence and absence of SCCNTs, respectively. Based on this analysis, we observe an increase in the electron transfer rate constant from 9.51×10^9 s^{-1} to 7.04×10^{10} s^{-1} as we decrease the particle diameter of CdSe from 4.5 to 3 nm. The electron transfer rate appears to be approximately eight times greater for the smaller 3 nm diameter quantum dots than the larger 4.5 nm quantum dots. As established in a previous study of CdSe−TiO_2 composites,[47] the higher energy conduction band in the smaller size quantum dots play a role in maximizing the electron transfer rate to the SCCNTs. A similar fast rate constant for electron transfer between excited CdSe and TiO_2[60] and SnO_2 has been measured by a transient grating technique.[61]

It should be noted the above estimate of the charge injection rate constant is an apparent value based on the average lifetimes and weighs both short and long components of the bleaching recovery. If we consider only the short lifetime components (τ_2 values in Table 1) we obtain an electron transfer rate constant from 1.2×10^{11} s^{-1} to 8.4×10^{11} s^{-1} as we decrease the particle diameter of CdSe from 4.5 to 3 nm. These values are nearly an order of magnitude greater than the one obtained by average lifetime analysis and represent an upper limit for the rate constant for the charge injection process. The magnitude of increase in the rate constant however is very similar (eight times) to the one obtained from average lifetime analysis. Both these analyses point out that the charge injection between excited CdSe and SCCNT is an ultrafast process and it can be modulated by controlling the particle size.

Photoelectrochemical Behavior of SCCNT−CdSe Composites. The transient absorption and emission studies indicate that the SCCNTs are quite effective in capturing electrons from excited CdSe nanocrystals. This conclusion is in agreement with earlier work[40] on captured electrons from H_2P-C_{60} systems. The ability to capture electrons from quantum dots thus paves the way for their use in photovoltaic applications. We cast films of CdSe, SCCNTs, and SCCNT−CdSe (as described above) on SnO_2−OTE to use as photoanodes in photoelectrochemical cells with platinum as a counter electrode and aqueous 0.1 M Na_2S as the electrolyte. Upon photoirradiation we observed a prompt generation of photocurrent as the photogenerated electrons are captured by SCCNTs and transported to the OTE electrode to generate photocurrent (Figure 10). The short circuit current response to incident Xe lamp light (>300 nm and 100 mW/cm^2) for the SCCNT−CdSe composite is significantly greater than that of SCCNT and CdSe films. The photocurrent response to repeated on−off cycles of

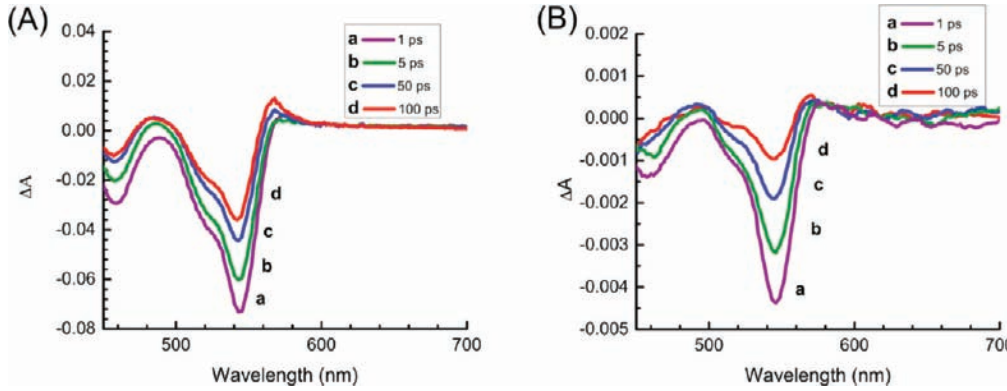

Figure 8. Time-resolved transient absorption spectra recorded following 387 nm laser pulse excitation of 4 nm diameter CdSe nanocrystals in THF/toluene/acetonitrile (1:1:4 v/v/v) suspension without (A) and with (B) the presence of SCCNTs.

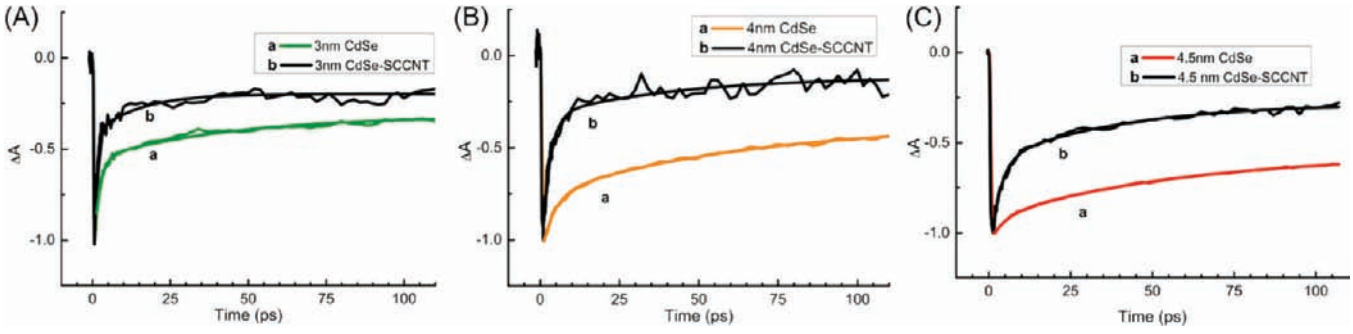

Figure 9. Transient absorption−time profiles of (A) 3, (B) 4.0, and (C) 4.5 nm CdSe nanocrystals. The traces were recorded in the absence (a) and presence (b) of SCCNTs. Double-exponential fits included. The monitoring wavelengths were at the bleaching maximum for the corresponding CdSe nanocrystals: (A) 498, (B) 547, and (C) 570 nm.

Table 1. Kinetic Analysis of CdSe Bleaching Recovery[a]

	CdSe (4.5 nm) at 570 nm	CdSe(4.5 nm)−SCCNT at 570 nm	CdSe (4 nm) at 547 nm	CdSe(4 nm)−SCCNT at 547 nm	CdSe (3 nm) at 498 nm	CdSe(3 nm)−SCCNT at 498 nm
a_1	−0.35	−0.32	−0.39	−0.22	−0.24	−0.23
τ_1 (ps) slow decay	64.12	43.76	62.24	42.31	43.74	14.12
a_2	−0.13	−0.58	−0.33	−0.88	−0.58	−1.68
τ_2 (ps) fast decay	4.68	2.99	3.86	2.45	1.88	0.73
$\langle\tau\rangle$ (ps)	62.51	39.29	59.30	34.67	39.85	10.45
R^2	0.9996	0.9956	0.9980	0.9775	0.9943	0.9587

[a] Biexponential fit parameters using eq 3 are listed. R^2 value included to show goodness of fit. Fitted lines are displayed with data in Figure 9.

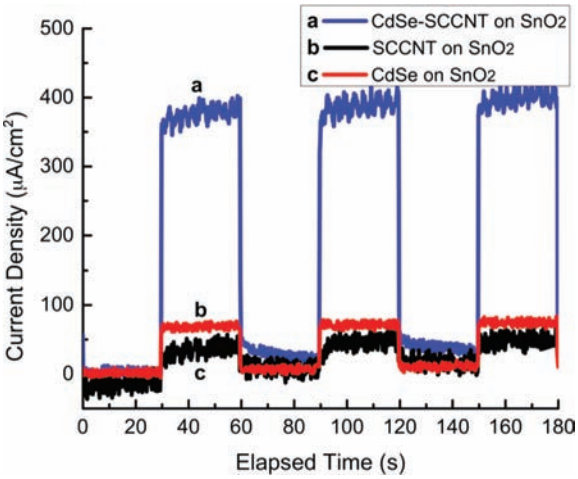

Figure 10. Photocurrent response of (a) CDSe−SCCNT, (b) SCCNT, and (c) CdSe films deposited on OTE/SnO_2 to ON−OFF cycles using white light (λ >300 nm and 100 mW/cm^2 Xe lamp) illumination. Platinum gauze was used as a counter electrode, and 0.1 M Na_2S as an electrolyte.

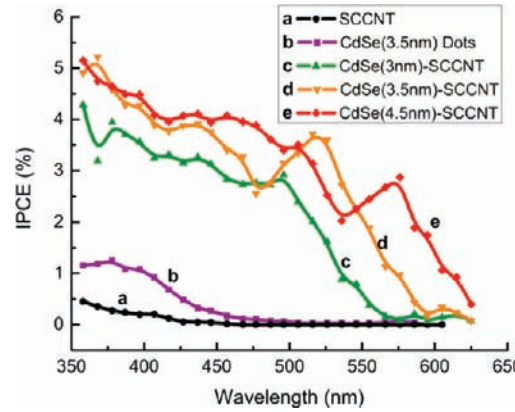

Figure 11. Dependence of the incident photon conversion efficiency on the incident wavelength for films cast on OTE: (a) SCCNT, (b) CdSe, (c) CdSe (3 nm)−SCCNT, (c) CdSe (3.5 nm)−SCCNT, and (c) CdSe (4.5 nm)−SCCNT. Electrolyte: 0.1 M Na_2S.

illumination shows the stability and reproducibility of the observed photocurrent in these systems.

The maximum photocurrent and open circuit voltage generated in the photochemical cell with >300 nm and 100 mW/cm^2 Xe lamp white light illumination were 0.4 mA/cm^2 and 0.2 V, respectively. The photocurrents observed for SCCNT−CdSe films were an order of magnitude higher than the currents generated by CdSe quantum dot solar cells and 3 orders of magnitude above those reported for CdSe dropcast solar cells.[62] The efficiency of SCCNTs in capturing and transporting electrons from CdSe quantum dots shows superior performance as compared to other carbon nanostructure based cells reported elsewhere.[20,36] SCCNT−CdSe cells show a 2-fold increase over CdSe−C_{60} devices[20] and a nearly 100-fold increase over SWCNT−CdS devices.[36]

Figure 11 shows the incident photon conversion efficiency (IPCE) or external quantum efficiency as a function of excitation wavelength for SCCNT−CdSe, CdSe, and SCCNT films. The IPCE values were determined using eq 6.

$$\mathrm{IPCE}(\%) = 100 \times (1240/\lambda) \times (I_{sc}/I_{inc}) \qquad (6)$$

where I_{sc} and I_{inc} represent short circuit current and incident light power at a specific wavelength, λ. The photocurrent response of SCCNT−CdSe quantum dots of three different diameters shows a size dependent photoresponse. The blue shift in the onset of photocurrent observed with decreasing particle size mirrors the absorption shift displayed in Figure 5. The IPCE values of single component films viz., CdSe and SCCNT (traces b and a in Figure 11), show a significantly lower response. The characteristic excitonic peaks at 570, 512, and 498 nm excitation for the 4.5, 3.5, and 3 nm diameter particles are also prominently displayed in the IPCE spectra in Figure 11. These observations thus confirm that the IPCE response is not a simple additive effect from the CdSe and SCCNT components, but rather a result of the unique interactions between the SCCNTs and CdSe quantum dots.

Mechanism of Photocurrent Generation. Previous studies have shown SCCNTs to be excellent electron acceptors with a Fermi level of −0.2 V vs NHE.[43] This energetic arrangement favors the quick electron transfer from excited CdSe particles. The electrons captured by the SCCNTs are quickly transported through the highly delocalized $\pi-\pi$ electron cloud of the stacked graphitic carbon sheets toward the collecting electrode surface. We deliberately coated the OTE with a thin layer of SnO_2 particles so as to increase the charge collection area of the electrode surface. The conduction band of SnO_2 is at 0 V vs NHE, which facilitates fast capture of electrons from the SCCNTs, leading to the generation of photocurrent (Figure 12).

(60) Shen, Q.; Katayama, K.; Yamaguchi, M.; Sawada, T.; Toyoda, T. *Thin Solid Films* **2005**, *486*, 15–19.
(61) Shen, Q.; Yanai, M.; Katayama, K.; Sawada, T.; Toyoda, T. *Chem. Phys. Lett.* **2007**, *442*, 89–96.
(62) Biebersdorf, A.; Dietmuller, R.; Susha, A. S.; Rogach, A. L.; Poznyak, S. K.; Talapin, D. V.; Weller, H.; Klar, T. A.; Feldmann, J. *Nano Lett.* **2006**, *6*, 1559–1563.

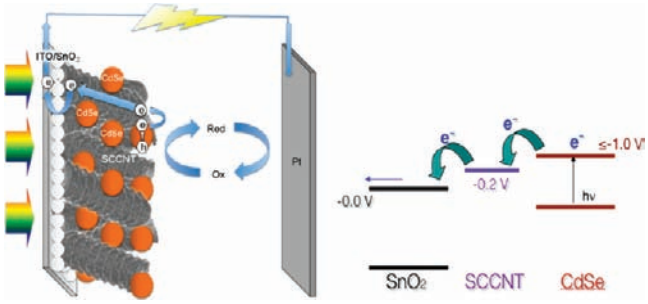

Figure 12. Mechanism of photocurrent generation in a SCCNT−CdSe based photoelectrochemical solar cell (Left) and energy level diagram (Right). All potentials listed are vs NHE (Normal Hydrogen Electrode).

The presence of sulfide/polysulfide ($S^{2-}/(S_n)^{2-}$) assists in the regeneration of CdSe nanocrystallites by scavenging the holes.

$$2\mathrm{CdSe}(h^+) + S^{2-}-(\mathrm{excess})S^{2-} \rightarrow \mathrm{CdSe} + (S_n)^{2-} \quad (7)$$

Although direct electron transfer between the excited SCCNT and the SnO_2 film is possible, contribution of this process as well as electron transfer between CdSe and SnO_2 to the overall photocurrent production is relatively small. The IPCE spectra a and b in Figure 11 support such an argument. Based on the IPCE and short circuit current measurements we can conclude that SCCNT serves as a scaffold architecture to facilitate capture and transport of photogenerated electrons from CdSe nanocrystals. A better dispersion of the CdSe nanocrystals is crucial for further maximizing the photoconversion efficiency of quantum dot solar cells. It should be noted that the observed IPCE values are lower than the one reported with TiO_2−CdSe composite films. Based on the UV−visible absorption characteristics of the SCCNT scaffold, the absorbance of the SCCNT in the composite structure is significant (~50%) and hence would limit the light absorption by the CdSe quantum dots. Although the charge injection rate from excited CdSe into the SCCNT is quite fast, the transport of electrons to the collecting electrode surface needs to be facilitated. The lower open circuit voltage will be a factor in determining the overall power conversion efficiency which in the present case is very low (<0.1%). As discussed in our earlier study, the Fermi level equilibration between the sensitizer and carbon nanotubes often drives the open circuit voltage lower than the one obtained with the sensitizer and TiO_2 films. Thus despite our success in the fast capture of electrons from excited CdSe by the SCCNT, the lower energy difference (and hence the open circuit potential) limits the overall photoelectrochemical performance of these solar cells. Further modifications of carbon nanotubes with semiconductor composites and/or functional groups are necessary to drive the Fermi level to more negative potentials.

Conclusion

Carbon nanostructures are well suited as conducting scaffolds as they collect electrons from excited semiconductor nanocrystals (CdSe quantum dots) and transport them to the conducting electrode surface. Thin films of CdSe dots alone show limitations in transporting the photogenerated electrons toward the electrode surface as evidenced by a nearly 10-fold increase in observed photocurrent upon the addition of SCCNTs to the photoanode. Excited state interaction between CdSe and SCCNT films is realized from the fast electron transfer between the two. Composites of CdSe quantum dots with stacked-cup carbon nanotubes provide a new and promising direction toward developing effective light energy harvesting strategies.

Acknowledgment. The research described herein was supported by the Office of Basic Energy Sciences of the U.S. Department of Energy. We would also like to thank Prof. Thomas Kosel for his assistance in TEM analysis, Cameron Postnikoff for setting up transient absorption experiments, and Brian Seger for his help in electrophoretic deposition. This is contribution number NDRL 4804 from the Notre Dame Radiation Laboratory.

Supporting Information Available: Experimental methodologies. This material is available free of charge via the Internet at http://pubs.acs.org.

JA903337C